JOC*Article*

Computational Strategies for Evaluating Barrier Heights for Gas-Phase Reactions of Lithium Enolates

Lawrence M. Pratt*

Department of Chemistry, Fisk University, 1000 17th Avenue North, Nashville, Tennessee 37209

Ngân Văn Nguỹên

University of Pedagogy, 280 An Duong Vuong, District 5, Hô Chí Minh City, Vietnam

B. Ramachandran

Department of Chemistry, Louisiana Tech University, Ruston, Louisiana 71272

lpratt@fisk.edu

Received February 22, 2005

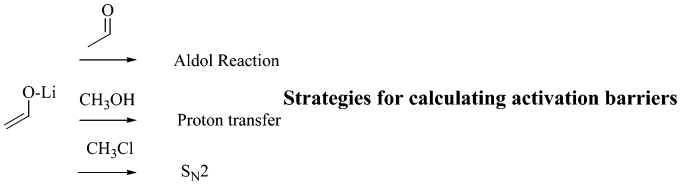

Gas-phase activation energies were calculated for three lithium enolate reactions by using several different ab initio and density functional theory (DFT) methods to determine which levels of theory generate acceptable results. The reactions included an aldol-type addition of an enolate to an aldehyde, a proton transfer from an alcohol to a lithium enolate, and an S_N2 reaction of an enolate with chloromethane. For each reaction, the calculations were performed for both the monomeric and dimeric forms of the lithium enolate. It was found that transition state geometry optimization with B3LYP followed by single point MP2 calculations generally provided acceptable results compared to higher level ab initio methods.

Introduction

Lithium enolates are among the most important reagents for carbon−carbon bond formation in organic synthesis, and they have been the subject of numerous theoretical and experimental investigations.[1−14] A major theoretical breakthrough was the development of pure and hybrid Density Functional Theory (DFT) computational methods, which include electron correlation at a fraction of the cost of MP2 and higher correlated methods. These methods have been used extensively to provide ground-state geometries and energies for a variety of organic lithium compounds in the gas phase, and in solution using microsolvation with explicit ethereal ligands and/or continuum solvent models.[15−25] The results of

(1) Pratt, L. M.; Streitwieser, A. *J. Org. Chem*. **2003**, *68*, 2830.
(2) Streitwieser, A.; Juaristi, E.; Kim, Y.-J.; Pugh, J. *Org. Lett*. **2000**, *2*, 3739.
(3) Kim, Y.-J.; Streitwieser, A. *Org. Lett*. **2002**, *4*, 573.
(4) Sun, C.; Williard, P. G. *J. Am. Chem. Soc*. **2000**, *122*, 7829.
(5) Uragami, M.; Tomioka, K.; Koga, K. *Tetrahedron*: *Asymmetry* **1995**, *6*, 701.
(6) Bunn, B. J.; Simpkins, N. S. *J. Org. Chem*. **1993**, *58*, 533.
(7) Jackman, L. M.; Haddon, C. *J. Am. Chem. Soc*. **1973**, *95*, 3687.
(8) Jackman, L. M.; Lange, B. C. *J. Am. Chem. Soc*. **1981**, *103*, 4494.
(9) Jackman, L. M.; Szeverenyi, N. M. *J. Am. Chem. Soc*. **1977**, *99*, 4954.
(10) Abu-Hasanayn, F.; Streitwieser, A. *J. Am. Chem. Soc*. **1996**, *118*, 8136.
(11) Henderson, K. W.; Dorigo, A. E.; Liu, Q.-Y.; Williard, P. G.; Schleyer, P. v. R.; Bernstein, P. R. *J. Am. Chem. Soc*. **1996**, *118*, 1339.
(12) Murakata, M.; Nakajima, M.; Koga, K. *J. Chem. Soc.*, *Chem. Commun*. **1990**, 1657.
(13) Hasegawa, Y.; Kawasaki, H.; Koga, K. *Tetrahedron Lett*. **1993**, *34*, 1963.
(14) Streitwieser, A.; Kim, Y. J.; Wang, D. Z.-R. *Org. Lett*. **2001**, *3*, 2599.
(15) Pratt, L. M.; Newman, A.; St. Cyr, J.; Johnson, H.; Miles, B.; Lattier, A.; Austin, E.; Henderson, S.; Hershey, B.; Lin, M.; Balamraju, Y.; Sammonds, L.; Cheramie, J.; Karnes, J.; Hymel, E.; Woodford, B.; Carter, C. *J. Org. Chem*. **2003**, *68*, 6387.
(16) Mogali, S.; Darville, K.; Pratt, L. M. *J. Org. Chem*. **2001**, *66*, 2368.
(17) Pratt, L. M.; Ramachandran, B.; Xidos, J. D.; Cramer, C. J.; Truhlar, D. G. *J. Org. Chem*. **2002**, *67*, 7607.
(18) Pratt, L. M.; Kass, S. R. *J. Org. Chem*. **2004**, *69*, 2123.
(19) Novak, I.; Pratt, L. M. *Chem. Phys. Lett*. **2004**, *400*, 558.
(20) Pratt, L. M.; Mu, R. *J. Org. Chem*. **2004**, *69*, 7519.
(21) Pratt, L. M.; Mu, R.; Jones, D. R. *J. Org. Chem*. **2005**, *70*, 101.
(22) Pratt, L. M. *Bull. Chem. Soc. Jpn.* In press.

10.1021/jo0503409 CCC: $30.25
Published on Web 00/00/0000

these calculations have generally been in agreement with available experimental data, and often generated results comparable to those of MP2 and higher level calculations. Modeling of transition structures and activation energies is a considerably more difficult problem. Electron correlation effects are especially important in obtaining accurate activation energies, making Hartree−Fock methods unreliable. Correlation is included in post Hartree−Fock methods such as MP2, MP4, QCISD, and coupled cluster methods, but since these methods generally scale as n^7, where n is the number of electrons, MP4 and higher methods are not practical for most systems of interest, and MP2 optimizations are possible only for systems of modest size. Although DFT methods do include electron correlation, they sometimes underestimate activation barriers,[26,27] and sometimes fail to predict an activation barrier at all. Despite these limitations, since the computational effort generally scales as N^4, where N is the number of atoms in the molecule, DFT methods are commonly used for the calculation of activation barriers for organolithium and other main group organometallic compounds.[28−32] The purpose of this study is to compare Hartree−Fock, DFT, and MP2 methods with the best available transition structure calculations in the gas phase to determine which levels of theory can be used to obtain accurate activation energies. Although organolithium compounds are generally used in solution, solvation is a complex issue and was not treated in this study. Rather, we focused on obtaining one or more acceptable gas-phase methods that will be suitable for use in conjunction with solvent models in the future.

Computational Methods

All geometry optimizations, transition structure searches, and frequency calculations were performed with the Gaussian 98 or Gaussian 03 programs.[33] Transition structures were located either with the QST3 method or by further optimization of a previously located transition structure at a different level of theory using the Opt=TS keyword. The reactants were taken as an optimized precomplex of the lithium enolate monomer or dimer with a coordinated acetaldehyde (aldol), methanol (proton transfer), or chloromethane molecule (S_N2). Three reactions of the lithium acetaldehyde enolate were modeled: an aldol-type reaction with a second acetaldehyde molecule; a proton-transfer reaction from methanol; and an S_N2 reaction with chloromethane. The reactions were each modeled via the lithium enolate monomer and dimer, as shown in Scheme 1. Geometry optimizations were performed at the following levels of theory for both the reactants and transition structures: HF/6-31+G(d), B3LYP/6-31+G(d), MPW1PW91/6-31+G(d), MP2/6-31+G(d), and for the monomers, QCISD/6-31+G(d). Single point energies were obtained at the MP4/6-31+G(d)//MP2/6-31+G(d), MP2/6-311+G(2df,2pd)//MP2/6-31+G(d), MP2/6-31+G(d,p)//MP2/6-31+G(d), and MP2/6-31+G(d)//B3LYP/6-31+G(d) levels of theory. Single point energies were also obtained to screen the newer MPW1K,[34] MPW1B95,[35] and MPW1BK[35] DFT methods as possible candidates for obtaining accurate activation energies. These energies were obtained at the MPW1PW91 geometries, except for the aldol monomer reaction, for which the B3LYP geometry was used as the MPW1PW91 method failed to locate a transition structure. Harmonic frequencies of the reactants and transition structures were calculated at the HF/6-31+G(d) level on HF/6-31+G(d) optimized geometries. The thermal corrections to the free energies at 298.15 K were taken from the frequency calculations and added to the internal energies at each level of theory, to obtain the free energies of each reactant and transition structure.

SCHEME 1. Aldol, Proton Transfer, and S_N2 Reactions of Lithium Enolates

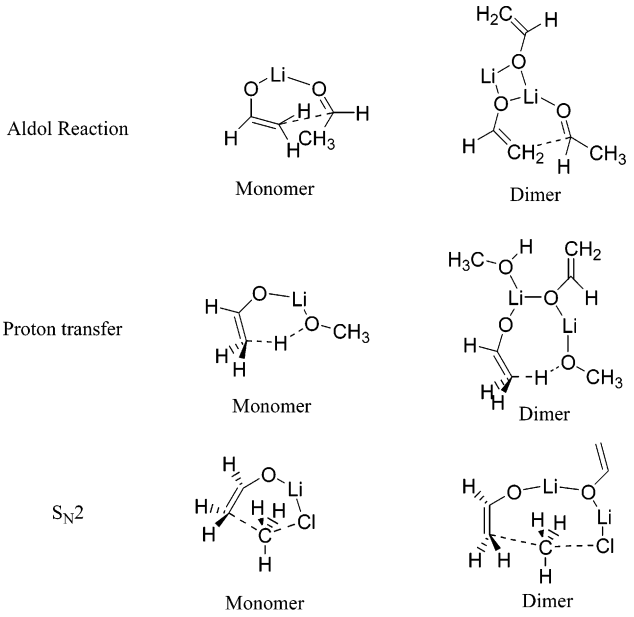

Results and Discussion

The calculated activation internal energies ($\Delta U^{\ddagger}$) and free energies ($\Delta G^{\ddagger}$) for the aldol reaction of the lithium acetaldehyde enolate monomer and dimer are shown in Tables 1 and 2, respectively. The MP2 optimized transition structures are shown in Figure 1. Optimization of the monomer at the QCISD/6-31+G(d) level located a transition structure with a partially formed C−C bond

(23) Pratt, L. M.; Ngan, V. N.; Ly, T. L. *J. Org. Chem*. **2005**, *70*, 2294.
(24) Prandt, P.; Haeffner, F. *J. Am. Chem. Soc*. **2003**, *125*, 48.
(25) Carlier, P. R.; Madura, J. D. *J. Org. Chem*. **2002**, *67*, 3832.
(26) Pugh, J. K.; Streitwieser, A. *J. Org. Chem*. **2001**, *66*, 1334.
(27) Gillies, M. B.; Tonder, J. E.; Tanner, D.; Norrby, P.-O. *J. Org. Chem*. **2002**, *67*, 7378.
(28) Pomelli, C. S.; Bianucci, A. M.; Crotti, P.; Favero, L. *J. Org. Chem*. **2005**, *69*, 150.
(29) Haeffner, F.; Houk, K. N.; Schulze, S. M.; Lee, J. K. *J. Org. Chem*. **2003**, *68*, 2310.
(30) Yamazaki, S.; Yamabe, S. *J. Org. Chem*. **2002**, *67*, 9346.
(31) Haeffner, F.; Brinck, T. *Organometallics* **2001**, *20*, 5134.
(32) Hasanayn, F.; Streitwieser, A.; Al-Rifai, R. *J. Am. Chem. Soc*. **2005**, *127*, 2249.
(33) Frisch, M. J.; Trucks, G. W.; Schlegel, H. B.; Scuseria, G. E.; Robb, M. A.; Cheeseman, J. R.; Montgomery, J. A., Jr.; Vreven, T.; Kudin, K. N.; Burant, J. C.; Millam, J. M.; Iyengar, S. S.; Tomasi, J.; Barone, V.; Mennucci, B.; Cossi, M.; Scalmani, G.; Rega, N.; Petersson, G. A.; Nakatsuji, H.; Hada, M.; Ehara, M.; Toyota, K.; Fukuda, R.; Hasegawa, J.; Ishida, M.; Nakajima, T.; Honda, Y.; Kitao, O.; Nakai, H.; Klene, M.; Li, X.; Knox, J. E.; Hratchian, H. P.; Cross, J. B.; Adamo, C.; Jaramillo, J.; Gomperts, R.; Stratmann, R. E.; Yazyev, O.; Austin, A. J.; Cammi, R.; Pomelli, C.; Ochterski, J. W.; Ayala, P. Y.; Morokuma, K.; Voth, G. A.; Salvador, P.; Dannenberg, J. J.; Zakrzewski, V. G.; Dapprich, S.; Daniels, A. D.; Strain, M. C.; Farkas, O.; Malick, D. K.; Rabuck, A. D.; Raghavachari, K.; Foresman, J. B.; Ortiz, J. V.; Cui, Q.; Baboul, A. G.; Clifford, S.; Cioslowski, J.; Stefanov, B. B.; Liu, G.; Liashenko, A.; Piskortz, P.; Komaromi, I.; Martin, R. L.; Fox, D. J.; Keith, T.; Al-Laham, M. A.; Peng, C. Y.; Nanayakkara, A.; Challacombe, M.; Gill, P. M. W.; Johnson, B.; Chem, W.; Wong, M. W.; Gonzalez, C.; Pople, J. A. *Gaussian 03*, Revision A.1; Gaussian, Inc.: Pittsburgh. PA, 2003.
(34) Lynch, B. J.; Fast, P. L.; Harris, M.; Truhlar, D. G. *J. Phys. Chem. A* **2000**, *104*, 4811.
(35) Zhao, Y.; Truhlar, D. G. *J. Phys. Chem. A* **2004**, *108*, 6908.

TABLE 1. Calculated Activation Barriers for the Aldol Reaction of the Lithium Acetaldehyde Monomer at 298.15 K[a]

level	$\Delta U^{\ddagger}$	$\Delta G^{\ddagger}$	C−C dist TS
HF/6-31+G*	11.1	15.6	2.160
B3LYP/6-31+G*	0.047	4.49	2.401
MPW1PW91/6-31+G*	no transition structure found		
MPW1K/6-31+G(d)// B3LYP/6-31+G(d)	−0.348	4.10	
MPW1B95/6-31+G(d)// B3LYP/6-31+G(d)	−0.284	4.16	
MPW1BK/6-31+G(d)// B3LYP/6-31+G(d)	−0.124	4.32	
MP2/6-31+G*	0.46	4.91	2.406
MP2/6-311+G(2df,2pd)// MP2/6-31+G*	−0.29	4.15	
MP4/6-31+G*// MP2/6-31+G*	2.15	6.60	
QCISD/6-31+G*	5.01	9.45	2.248

[a] Energies are in kcal/mol and bond distances are in Å.

TABLE 2. Calculated Activation Barriers for the Aldol Reaction of the Lithium Acetaldehyde Dimer at 298.15 K[a]

level	$\Delta U^{\ddagger}$	$\Delta G^{\ddagger}$	C−C dist TS
HF/6-31+G*	17.1	21.3	2.006
B3LYP/6-31+G*	5.76	10.0	1.956
MPW1PW91/6-31+G*	2.69	6.94	2.029
MPW1K/6-31+G(d)// MPW1PW91/6-31+G(d)	3.76	7.80	
MPW1B95/6-31+G(d)// MPW1PW91/6-31+G(d)	3.23	7.47	
MPW1BK/6-31+G(d)// MPW1PW91/6-31+G(d)	3.93	8.17	
MP2/6-31+G*	6.72	11.0	1.984
MP4/6-31+G*// MP2/6-31+G*	7.49	11.7	

[a] Energies are in kcal/mol and bond distances are in Å.

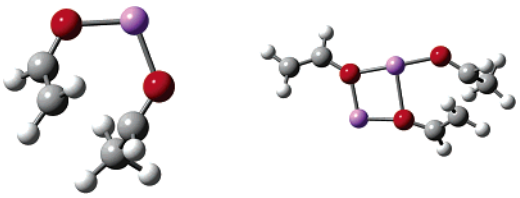

FIGURE 1. Optimized transition structures [MP2/6-31+G(d)] for the lithium acetaldehyde enolate aldol reaction: (left) monomer; (right) dimer—gray, carbon; white, hydrogen; red, oxygen; violet, lithium.

of 2.248 Å. Using the QCISD energy as the best available, it was observed that the Hartree−Fock calculation overestimated the activation energy by about 6 kcal/mol. In contrast, the B3LYP method underestimated the barrier by nearly 5 kcal/mol, and the MPW1PW91 method failed to locate a barrier at all. The activation internal energy with the B3LYP method was less than 0.05 kcal/mol, and nearly all the calculated free energy barrier came from the thermal contributions to the enthalpy and entropy. The single point MPW1K, MPW1B95, and MPW1BK DFT calculations each generated slightly negative $\Delta U^{\ddagger}$ values. The MP2/6-31+G(d) calculation fared only slightly better than B3LYP, and the MP2/6-311+G(2df,2pd) single point calculations resulted in an apparent negative internal energy of activation. However, the single point MP4/6-31+G(d)//MP2/6-31+G(d) activation internal energy was within 3 kcal/mol of the QCISD value. The newly forming C−C bond distance was nearly identical in the B3LYP and MP2 calculations, which was about 0.15 Å longer than that in the QCISD optimized geometry.

TABLE 3. Calculated Activation Barriers for the Proton Transfer Reaction of the Lithium Acetaldehyde Monomer at 298.15 K[a]

level	$\Delta U^{\ddagger}$	$\Delta G^{\ddagger}$	C−C dist TS	C−O dist TS
HF/6-31+G*	16.1	13.0	1.390	1.250
B3LYP/6-31+G*	6.23	3.10	1.375	1.290
MPW1PW91/6-31+G*	5.81	2.68	1.351	1.300
MPW1K/6-31+G(d)// MPW1PW91/6-31+G(d)	7.52	4.39		
MPW1B95/6-31+G(d)// MPW1PW91/6-31+G(d)	7.37	4.24		
MPW1BK/6-31+G(d)// MPW1PW91/6-31+G(d)	8.60	5.46		
MP2/6-31+G*	8.62	5.48	1.350	1.310
MP2/6-311+G(2df,2pd)// MP2/6-31+G*	9.71	6.58		
MP4/6-31+G*// MP2/6-31+G*	8.81	5.68		
QCISD/6-31+G*	10.6	7.44	1.376	1.280

[a] Energies are in kcal/mol and bond distances are in Å.

TABLE 4. Calculated Activation Barriers for the Proton Transfer Reaction of the Lithium Acetaldehyde Dimer at 298.15 K[a]

level	$\Delta U^{\ddagger}$	$\Delta G^{\ddagger}$	C−C dist TS	C−O dist TS
HF/6-31+G*	25.0	20.7	1.338	1.290
B3LYP/6-31+G*	14.0	9.75	1.281	1.390
MPW1PW91/6-31+G*	16.1	11.8	1.325	1.300
MPW1K/6-31+G(d)// MPW1PW91/6-31+G(d)	13.7	9.46		
MPW1B95/6-31+G(d)// MPW1PW91/6-31+G(d)	14.7	10.5		
MPW1BK/6-31+G(d)// MPW1PW91/6-31+G(d)	15.7	11.5		
MP2/6-31+G*	17.8	13.5	1.264	1.410
MP4/6-31+G*// MP2/6-31+G*	17.8	13.5		

[a] Energies are in kcal/mol and bond distances are in Å.

The calculated transition structure C−C bond distances in the dimer were all within about 0.07 Å of each other. As this system was too large for a QCISD calculation, the best available energy was taken as the MP4/6-31+G(d)//MP2/6-31+G(d) value. This was only 0.7 kcal/mol higher than the MP2 calculated result, and nearly 10 kcal/mol lower than that of the Hartree−Fock calculation. As with the monomer, each of the DFT methods underestimated the activation barrier, and the best DFT energy was obtained with the B3LYP method.

The calculated activation energies for proton transfer from a coordinated methanol molecule to the lithium enolate monomer are given in Table 3, and the corresponding energies for the dimer are in Table 4. Compared to the aldol reaction, the partially formed C−H bond lengths in the monomer varied much less with the level of theory, with the Hartree−Fock method generating the longest bond length and the MP2 method generating the shortest. Once again taking the QCISD results as the best available, the Hartree−Fock method was found to overestimate the activation internal energy by nearly 6 kcal/mol, and the B3LYP and MPW1PW91 methods underestimated that value by about 4 kcal/mol. With this reaction, however, the MPW1K, MPW1B95, and MPW1BK

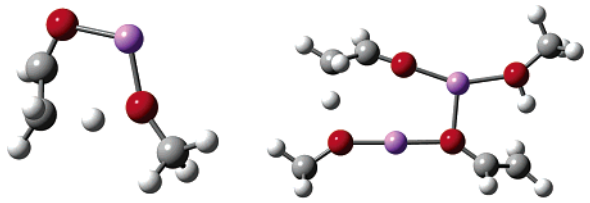

FIGURE 2. Optimized transition structures [MP2/6-31+G(d)] for the lithium acetaldehyde enolate proton-transfer reaction: (left) monomer; (right) dimer.

TABLE 5. Calculated Activation Barriers for the S_N2 Reaction of the Lithium Acetaldehyde Monomer at 298.15 K[a]

level	$\Delta U^{\ddagger}$	$\Delta G^{\ddagger}$	C−C dist TS
HF/6-31+G*	29.1	32.0	2.482
B3LYP/6-31+G*	18.8	21.7	2.459
MPW1PW91/6-31+G*	1.28	4.22	2.449
MPW1K/6-31+G(d)// MPW1PW91/6-31+G(d)	25.0	27.9	
MPW1B95/6-31+G(d)// MPW1PW91/6-31+G(d)	21.3	24.3	
MPW1BK/6-31+G(d)// MPW1PW91/6-31+G(d)	24.5	27.4	
MP2/6-31+G*	26.4	29.3	2.360
MP2/6-311+G(2df,2pd)// MP2/6-31+G*	24.2	27.1	
MP4/6-31+G*// MP2/6-31+G*	24.9	27.8	
QCISD/6-31+G*	27.4	30.4	2.410

[a] Energies are in kcal/mol and bond distances are in Å.

methods were all superior to B3LYP, with the MPW1BK method generating a barrier height nearly identical with that obtained by the MP2 method. The MP2 optimization with the 6-31+G(d) basis set underestimated the barrier by only 2 kcal/mol, and both the MP4/6-31+G(d) and MP2/6-311+G(2df,2pd) single point energies resulted in a modest improvement in the calculated barrier height.

The proton transfer reaction of the dimer showed a slightly larger spread of calculated lengths of the partially formed C−H bond with the level of theory. As with the monomer, the Hartree−Fock method significantly overestimated the activation barrier, and the MP2/6-31+G(d) optimization and the MP4/6-31+G(d) single point energy produced nearly identical barrier heights. Each of the DFT methods generated comparable barrier heights, which were 2−4 kcal/mol lower than those obtained by MP2. The MP2 optimized transition structures are shown in Figure 2.

The calculated activation barriers for the S_N2 reaction of the lithium acetaldehyde enolate monomer and dimer with chloromethane are shown in Tables 5 and 6, respectively. The MP2 optimized transition structures are shown in Figure 3. For the reaction via the lithium enolate monomer, the MP2/6-31+G(d) optimization generated the shortest partially formed C−C bond at 2.360 Å, compared to 2.4−2.5 Å with the other methods. However, the MP2/6-31+G(d) method generated an activation barrier only 1 kcal/mol lower than the QCISD/6-31+G(d) optimization, which was slightly better than the MP2/6-311+G(2df,2pd) and MP4/6-31+G(d) single point energies. As with the aldol and proton-transfer reactions, the activation barrier was overestimated by the Hartree−Fock method. The DFT methods showed a

TABLE 6. Calculated Activation Barriers for the S_N2 Reaction of the Lithium Acetaldehyde Dimer at 298.15 K[a]

level	$\Delta U^{\ddagger}$	$\Delta G^{\ddagger}$	C−C dist TS
HF/6-31+G*	28.5	31.2	2.494
B3LYP/6-31+G*	18.9	21.7	2.539
MPW1PW91/6-31+G*	20.1	22.8	2.464
MPW1K/6-31+G(d)// MPW1PW91/6-31+G(d)	23.1	25.9	
MPW1B95/6-31+G(d)// MPW1PW91/6-31+G(d)	21.1	23.9	
MPW1BK/6-31+G(d)// MPW1PW91/6-31+G(d)	23.3	26.0	
MP2/6-31+G*	24.3	27.0	2.366
MP4/6-31+G*// MP2/6-31+G*	23.6	26.4	

[a] Energies are in kcal/mol and bond distances are in Å.

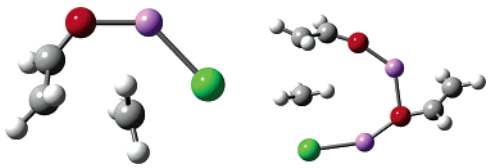

FIGURE 3. Optimized transition structures [MP2/6-31+G(d)] for the lithium acetaldehyde enolate S_N2 reaction: (left) monomer; (right) dimer.

wide disparity in the calculated activation barriers. The MPW1PW91 method predicted an internal energy of activation of only 1.3 kcal/mol, although the calculated length of the forming C−C bond was comparable to that of the B3LYP and MP2 methods. B3LYP underestimated the barrier by more than 8 kcal/mol, compared to the MP2 result, while the MPW1K, MPW1B95, and MPW1BK calculations generated similar results to each other, underestimating the barrier by 1−5 kcal/mol.

For the S_N2 reaction of the lithium enolate dimer, the variation of the forming C−C bond length with the computational method was similar to that of the monomer, with the MP2 method producing the shortest bond length. Once again, the MP2 optimization and MP4 single point calculations generated similar activation barriers, which were lower than those obtained by the Hartree−Fock calculation, and higher than those obtained by the DFT methods. The MPW1K and MPW1BK DFT methods performed the best in this case, underestimating the barrier height by only about 1 kcal/mol, compared to MP2, while the B3LYP, MPW1PW91, and MPW1B95 methods gave comparable results to each other, with activation barriers 3−5 kcal/mol lower than the MP2 values.

The data in Tables 1−6 show that the MP2 calculated activation barriers are generally in qualitative agreement with those calculated by using the MP4 or QCISD methods. In contrast, the B3LYP, MPW1PW91, MPW1K, MPW1B95, and MPW1BK calculations generated activation barriers that were erratic. In some cases the DFT results were in reasonable agreement with the MP2 energies, and in other cases, they severely underestimated the barriers, or even failed to locate a transition structure at all. However, when a transition structure was located, the lengths of the forming or breaking bonds were generally in good agreement with the MP2 calculations. This fact raised the question as to whether good results could be obtained from single point MP2 energies

TABLE 7. Comparison of $\Delta U^{\ddagger}$ [$\Delta G^{\ddagger}$] at the MP2/6-31+G(d) and MP2/6-31+G(d)//B3LYP/6-31+G(d) Levels of Theory at 298.15 K[a]

reaction	aggregate	MP2/6-31+G(d)	MP2/6-31+G(d)//B3LYP/6-31+G(d)
aldol	monomer	0.46 [4.91]	2.24 [6.69]
aldol	dimer	6.72 [11.0]	5.78 [10.0]
proton transfer	monomer	8.62 [5.48]	8.64 [5.50]
proton transfer	dimer	17.8 [13.5]	18.1 [13.8]
S_N2	monomer	26.4 [29.3]	26.9 [29.8]
S_N2	dimer	24.3 [27.0]	23.9 [26.7]

[a] Energies are in kcal/mol and bond distances are in Å.

on B3LYP geometries. The results are shown in Table 7. Comparison of the barrier heights shows that the two methods agree within 1 kcal/mol, with the exception of the aldol reaction via the lithium enolate monomer, for which the two results differed by about 1.8 kcal/mol. While geometry optimization at the MP2 level is preferable, it is not always practical when large molecules are involved, especially those where solvent ligands are included. Thus, provided that a transition structure can be found with the B3LYP method, single point MP2 energies at the B3LYP geometries provide a reasonable estimate of lithium enolate activation barriers in the gas phase.

Conclusions

Activation barriers for lithium enolate reactions were calculated for both the monomer and dimer at several levels of theory. Geometry optimizations at the QCISD/6-31+G(d) level and MP4/6-31+G(d)//MP2/6-31+G(d) single point calculations provided the highest level of theory that is currently practical for reaction barriers of the enolate monomer and dimer, respectively. Hartree−Fock methods invariably overestimated the activation barriers, and in most cases, the barriers were underestimated by each of the DFT methods. The DFT errors were sometimes large, and in one case, the MW1PW91 method failed to locate an activation barrier at all. In other cases some of the DFT methods generated activation barriers comparable to those obtained by MP2. The large variation in the performance of the DFT methods indicates that they should be treated as semiempirical methods for the calculation of activation barriers: Sometimes they work, sometimes they do not, and they should be used with caution until their performance can be further evaluated for a large number of organolithium reactions. In most cases, MPW1K, MPWB1K, and MPW1B95 gave better results than B3LYP or MPW1PW91, suggesting that these methods do yield improved results for reactions very different from those that were used for their parametrization. The MP2 method did provide reasonable geometries in most cases, and single point MP2 calculations at the B3LYP geometries provided qualitatively correct activation barriers.

Acknowledgment. This work was supported in part by the NSF grant no. CHE-0139076. The authors thank Christopher J. Cramer at the University of Minnesota for helpful discussions.

Supporting Information Available: Tables of optimized geometries and energies of all reactants and transition structures. This material is available free of charge via the Internet at http://pubs.acs.org.

JO0503409